Stresses in the Blades of a Cargo Ship Propeller

H. G. KEIL*
Hamburg University, Hamburg, West Germany

AND

J. J. BLAUROCK† AND E. A. WEITENDORF‡
Hamburg Model Basin, Hamburg, West Germany

The problem of propeller-blade failures on a single-screw ship of the "Lichtenfels" class is solved by full-scale measurements, model tests and a calculation with elementary theory. The results show that the failures are caused by wake-induced forced oscillations of the blades. The agreement of the results of the three investigations is acceptable. It is further shown by model tests in regular and irregular waves that the stresses in a seaway can be much higher than those in smooth water.

Introduction

DURING recent years a number of propeller-blade failures have occurred, both in Germany and abroad. The investigations reported below were initiated by two propeller-blade failures on single-screw ships of the "Lichtenfels" class. The preliminary results obtained from the measurements made on the "Neuenfels" were reported at last year's meeting of the Schiffbautechnische Gesellschaft Committee on Ship Vibration. The full results of the investigation are given below.

The practical solution to this particular problem proved to be the reduction in the propeller diameter D to 4.50 m, and an increase in the thickness of the blade sections; the object of the investigations was not merely to establish the causes of the propeller-blade failures in the "Lichtenfels" class ships, but also to study the possibility of determining at the design stage whether the propeller blades will be subjected to excessively high loadings. There are two possible ways of doing this: 1) calculation of the dynamic propeller-blade loading and stresses using the nominal wake distribution as determined by a model test; and 2) measurement of the blade stresses on a model propeller working behind the model hull. These two types of investigation have been made for the propeller of the "Neuenfels." The results obtained are compared with those obtained on the full scale. In addition further experiments, which are easier to perform in the towing tank than on the full-scale, were carried out when making the stress measurements on the model.

Table 1 Ship data

Length, bp	L_{pp}	= 128.70 m
Breadth, moulded	B_{sp}	= 17.80 m
Design draught	T_{kr}	= 8.00 m
Block coefficient for T_{kr} = 8.00 m	δ	= 0.681
Draught during tests:		
Draught, forward	T_v	= 3.35 m
Draught, aft	T_h	= 5.98 m

Received May 28, 1971; revision received July 8, 1971. Condensed from the paper presented at the Annual Meeting of Schiffbautechnische Gesellschaft, Berlin, Nov. 1970.

Index category: Marine Vessel Design (Including Loads); Marine Vessel Vibration.

* Research Scientist, Institut fuer Schiffbau.
† Research Scientist.
‡ Research Scientist.

Ship and Propeller Data

The ship data are given in Table 1. The main propulsion machinery comprises a two-stroke cross-head engine (Table 2). As to the propeller data of ship and model see Table 3.

Full-Scale Measurements

1. Instrumentation

The leads connected to the resistance strain gages on the propeller blades were housed in grooves cut on the face of the blades, and like the strain gauges themselves these leads were covered with sealing material and plastic metal. To enable an adequate impression to be gained of the stress distribution over the propeller blade, measurements were taken at various radii on both the face and the back of the blade and at various positions along the chord. To check that the results obtained were reproducible and that the blades were uniformly loaded, certain of the measuring points were repeated on more than one blade (Fig. 1).

As a result there was a total of 30 measuring points: 23 strain gages or 45° strain gage rosettes on the blades; 3 strain gages on the propeller shaft to measure thrust variation, torque, and torque variation; 3 piezoelectric accelerometers on the blades; and a 1 piezoelectric accelerometer arranged axially on the end of the shaft. The strain gages fitted to the blades were of the 120-ohm type, those on the shaft were of the 600-ohm type. A detailed description of the way in which the strain ages were mounted and sealed and of the arrangement of the leads is given in Ref. 2.

2. Evaluation

The results were evaluated by digital methods. At the lower speeds up to 80 rpm the readings were taken over 20 revolutions, and at the higher speeds over 40 revolutions. The following were calculated from the recorded results: a) the mean strain; b) the extreme values of the strain; c) the Fourier spectra of the strain up to the 20th order.

Table 2 Main propulsion machinery

Type	M.A.N. K6Z 70/120 D
Output	Ne = 7200 hp
Speed	n = 135 rpm

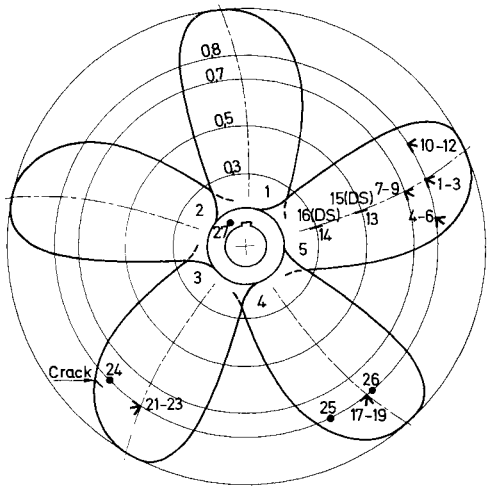

Fig. 1 Measuring points on full-scale propeller.

a) Mean strain

The mean strains were determined by means of two completely independent methods. In one of these they were taken as the mean value of the total of 20 × 96 or 40 × 96 readings relative to the absolute zero of the "total value measurement." In the second method the mean strains were determined from the "measurement of variations." In this measurement the absolute amplifier zero was turned down by a compensation circuit and recorded. The sum of this value and of the mean value given by the Fourier analysis gave the required mean value. The results obtained by these two methods are plotted as open and solid points on the lines for the mean strain shown on the diagrams giving the total values.

b) Extreme values of strain

The extreme values of the strains were determined only from the "total value measurement." The maximum and minimum values for each revolution were determined and the mean values of the 20 or 40 extreme values obtained in this way were then calculated.

c) Fourier spectra of the strain

The results obtained from the "measurement of variations" were analyzed up to the 20th order. Each revolution was analyzed, and the mean spectrum was calculated from the 20 or 40 spectra obtained in this way. A second possible method would be to average out the data, i.e., to determine the average values of the 20 or 40 readings obtained for each of the 96 points, and then to calculate a spectrum for the mean data. The first method involves considerably more calculation, but was used in this case. The results for some of the

Table 3 Propeller data

Full scale:	
Diameter	D = 4700 mm
Pitch	P_m = 4080 mm
Blade-area ratio	A_e/A_0 = 0.61
Number of blades	z = 5
Material	Cu-Al-Ni special bronze alloy
Modulus of elasticity	$E = 1.26 \times 10^6$ kp/cm²
Fatigue strength in sea-water for 20×10^6 load cycles	1350 kp/cm²
Model:	
Scale	$\lambda = 20$
Material	Brass
Modulus of elasticity	$E = 1.05 \times 10^6$ kp/cm²

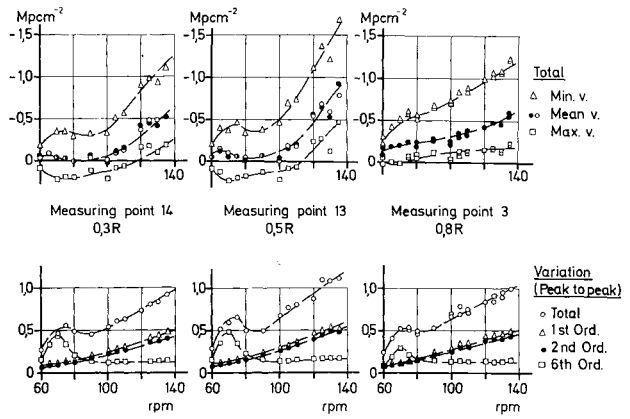

Fig. 2 Radical distribution of stresses at the thickest part of the blade, full-scale.

measuring points were also evaluated by the second method. The results showed that a collection of 20 or 40 readings was considerably too small for obtaining the means of the data to enable the phases to be determined with sufficient accuracy. The errors are less so far as the determination of the amplitude is concerned.

3. Results

The illustrations show the stresses plotted against the speed, one diagram giving the minimum, maximum, and mean values, and another diagram showing the total variation together with the double (peak to peak) amplitudes of the first, second, and sixth orders of the propeller speed.

The stress scale is derived from the value of 1.26×10^6 kp/cm² for the Modulus of Elasticity at 20×10^6 load cycles as given by the propeller manufacturer.

A comparison of the radial stresses at the various radii as shown in Fig. 2 indicates clearly that the maximum stresses in the material occur neither at the blade root nor at the blade tip. It is shown in Fig. 3 that the stresses can attain appreciable values at the leading edge, and that they then increase further towards the thickest part of the blade, dropping away to very low values at the trailing edge.

Unfortunately the failure of the instrumentation at measuring point 15 enables the stresses on the back of the blade to be compared with those on the face only at $x = 0.3$ (Fig. 4). Here the stresses are approximately the same at the lower speeds, but become clearly higher on the back of the blade at the higher speeds.

All the radial stresses have the following features in common: a) the maximum values and the variations are at a relative maximum at the critical speed of about 70 rpm, and increase with increasing speed. b) the effects of the first and second order, which result from the wake, become dominant

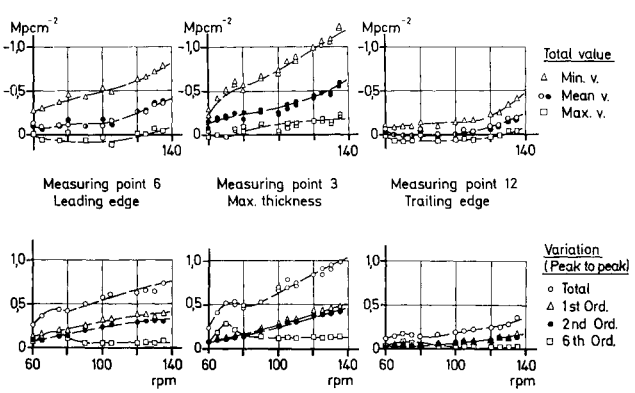

Fig. 3 Distribution of stresses along the chord at x = 0.8, full-scale.

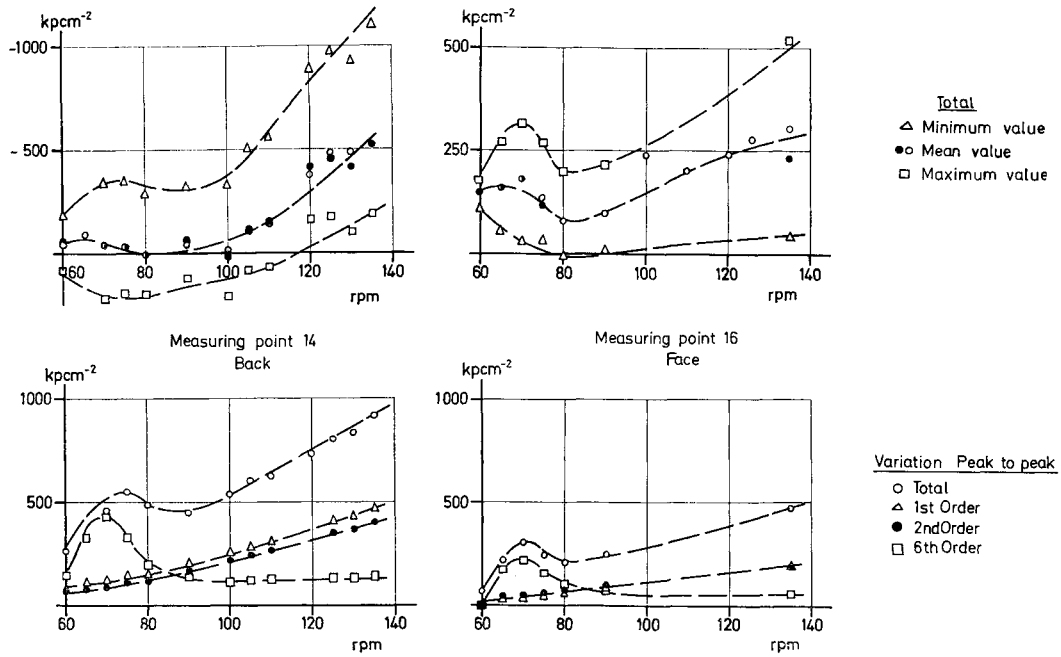

Fig. 4 Stresses on the face and on the back at $x = 0.3$, full-scale.

as the speed increases. Only at the lower speeds is the excitation by the six-cylinder main engine significant. Figure 5 compares the principal stress as calculated from the stresses in three directions recorded at measuring points 1–3 with the radial stress. The maximum difference amounts to 10%.

Calculations

In order to investigate the blade stresses theoretically it was necessary to know the wake distribution in the plane of the propeller. To determine this, measurements of the nominal axial wake were made on a model of the "Neuenfels" at a draught corresponding to that of the trial trip ($T_v = 3.35$ m; $T_h = 5.98$ m). The wake isotachs are shown in Fig. 6. Using the results of these measurements the hydrodynamic excitations of the propeller blades were then calculated by the method proposed by Krohn and Schwanecke,[3–5] only the first five harmonics being taken into account. Since the loads predicted by this method of calculation are inevitably too high, a reduction factor C_{km} was introduced; this was derived from results given by Breslin (Ref. 6, Fig. 4). This determines the ratio of the unsteady three-dimensional lift to the unsteady two-dimensional lift for aerofoils at the same reduced frequency $k = \omega \cdot C/2V$. The five calculated harmonics of the speed were multiplied by this reduction factor $C_{km} = L'_{3dim}/L'_{2dim}$, which has to be applied to each harmonic component separately. Calculations of the vibratory stresses in propeller blades due to the hydrodynamic excitation forces referred to above have been carried out by Pfuetzner[7] and Boese[8]; both of whom employed a constant value of $C_{km} = 0.66$ for the reduction factor for all orders of vibration. Pfuetzner used the transfer matrix method, the propeller blade being regarded as a plane beam rigidly clamped at one end and an average pitch being assumed. This simplification was not adopted by Boese, whose calculations were performed using the Guembel-Csupor method. The assumption made in these calculations, that the centroids of the individual blade sections lie on a straight line, was investigated by Blume.[9] It was found that the center of thrust is not significantly displaced from the centroid of the blade section. The major part of the torsional moment that is present is due to the rake of the sections.

The natural frequencies of vibration of the "Neuenfels" propeller were calculated using the computer program established by Blume. He extended the Boese calculation methods to include the torsion, a value of $K = 0.66$ being as-

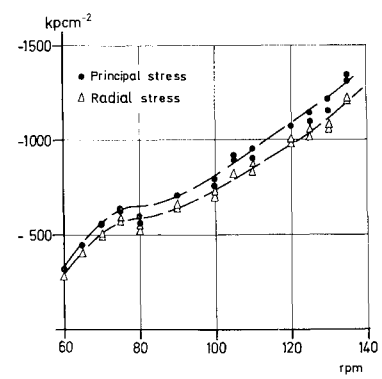

Fig. 5 Principal stresses at $x = 0.8$, full-scale.

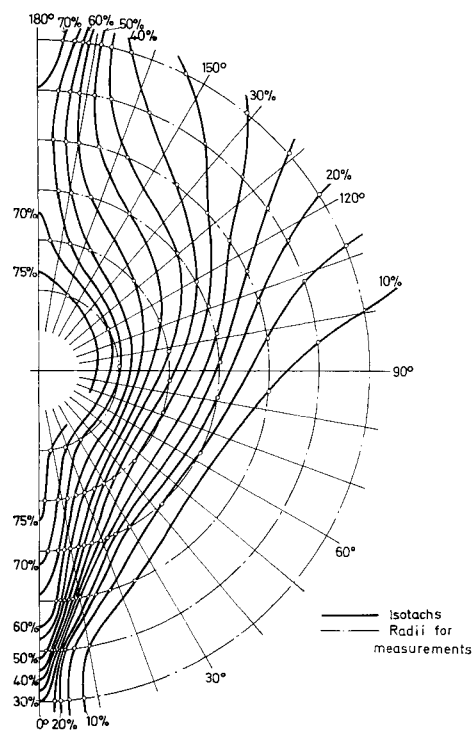

Fig. 6 Wake isotach lines, model.

Table 4 Section modulus differences between ship and model, back of blade

Radius x	0.3	0.4	0.5	0.6	0.7	0.8
Percent	3.8	4.6	6.8	9.8	9.5	11.6

sumed for the reduction factor for the hydrodynamic masses. With the torsion taken into account the first order natural frequency was found to be $f_0 = 18.69$ cps.

At the same time the forced vibrations were calculated by means of the program, use being made of the hydrodynamic excitation loads reduced in the manner described above. The mean values of the stresses were calculated by the simplified method due to Conolly[10] using the precise values of the Section Modulus of the profiles. The results are given in the Sec. "Comparison of the Results of the Full-Scale Tests, Calculations, and Model Tests."

Model Tests

The results of the full-scale tests showed clearly that the principal dynamic loading on the propeller blades is of hydrodynamic origin. It was therefore possible to carry out model tests based on the Froude Law of Similarity which would at the same time indicate whether stress measurements of this type performed on the model propeller would be likely to yield useful results.

Because of the shortage of time, the stress measurements that are described below were carried out on a model of one of the last propeller designs to be investigated with a view to modernizing the "Lichtenfels" class. The differences between the model propeller and that fitted to the ship were very minor, and amounted only to a difference in the Section Modulus values. The values of the Section Modulus of the model employed exceeded those of the full-scale propeller by the amounts given in Table 4. These percentage increases in the Section Modulus were allowed for when evaluating the model test results.

1. Instrumentation

Since use was to be made of existing equipment for transferring the readings from the propeller to the recorders it was not possible to take readings at more than nine points without making major modifications. A suitable selection was therefore made of the points at which readings had been taken on the full-scale propeller (Fig. 7). Semiconductor strain gages having a gage factor of about 100 and an active gage length of 1.5 mm were used. The active semiconductor strain gages on the propeller blades were connected into a full bridge circuit together with a temperature compensation gage (also a semiconductor) and two normal metal-film strain gages. The resistance of all the gages amounted to 120 ohms.

In addition to the smooth water tests run at draughts corresponding to the trial trip conditions of the full-scale ship, a number of special tests were made. In an irregular seaway the corresponding propeller speed with a head sea was $n = 128$ rpm, and with a following sea $n = 123$ rpm. The main characteristics of this irregular seaway are listed in Table 5. This model seaway corresponds to a fully developed seaway on the North Atlantic at a wind force of about $7\frac{1}{2}$ Beaufort.

Table 5 Characteristics of irregular model seaway

Mean wave height	H_m	= 3.32 m
Mean value of $\frac{1}{3}$ highest waves	$H_{1/3}$	= 4.50 m
Mean value of $\frac{1}{10}$ highest waves	$H_{1/10}$	= 5.86 m
Maximum wave height	H_{max}	= 8.16 m
Mean wave period	τ_m	= 7.02 sec
Mean value of $\frac{1}{3}$ longest periods	$\tau_{1/3}$	= 7.96 sec
Mean value of $\frac{1}{10}$ longest periods	$\tau_{1/10}$	= 8.59 sec
Maximum wave period	τ_{max}	= 9.57 sec

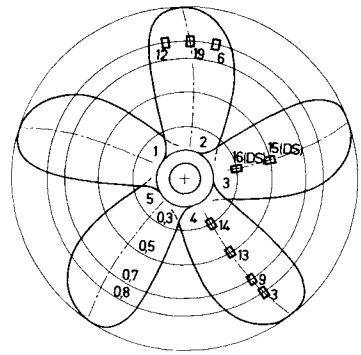

Fig. 7 Measuring points on the model propeller.

In order to obtain the same torque coefficient K_Q on the model as on the full-scale ship, a friction reduction calculated in accordance with the recommendations of the ITTC was applied to the model. In the case of the tests performed in a seaway the wind force component for the above-water portion of the hull was added to this.

2. Evaluation and Extrapolation to Full-Scale

The measured readings that were recorded in analog form on a magnetic tape were evaluated in digital form on a data processing unit. The average values of 96 readings per revolution were determined over a total of 40 revolutions. From these the Fourier coefficients were calculated from the zero (mean value) to the eleventh order. At the same time the maximum and minimum values per revolution of the 96 readings for which averages were obtained were printed out. This was the method of evaluation employed for the smooth-water tests; in the case of the tests carried out in irregular waves the calculations were performed for every fourth revolution.

Since the Modulus of Elasticity for the model propeller was known there was no difficulty in determining the stresses from the measured strains. The extrapolation of the model stresses to the full scale was effected by means of the Froude Law of Similarity. Since the results of the full-scale tests had shown that the principal dynamic loading of the propeller blades is hydrodynamic in origin, the use of this method of extrapolation appears justified. The Cauchy Law of Similarity for the transformation of natural frequencies can therefore be disregarded.

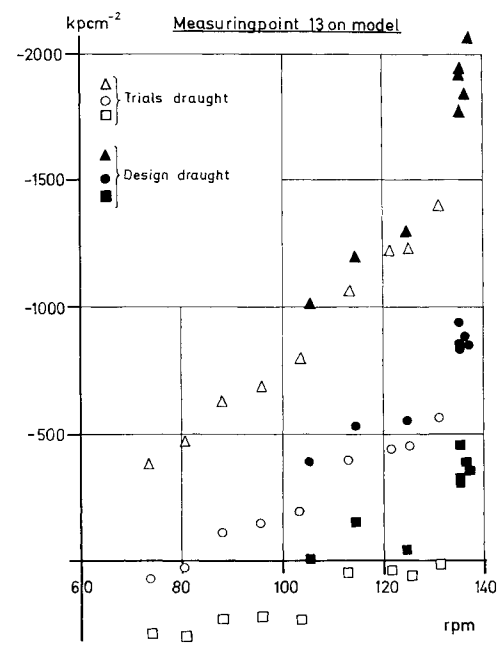

Fig. 8 Stresses at x = 0.5 obtained at design draught and at trials draught, model.

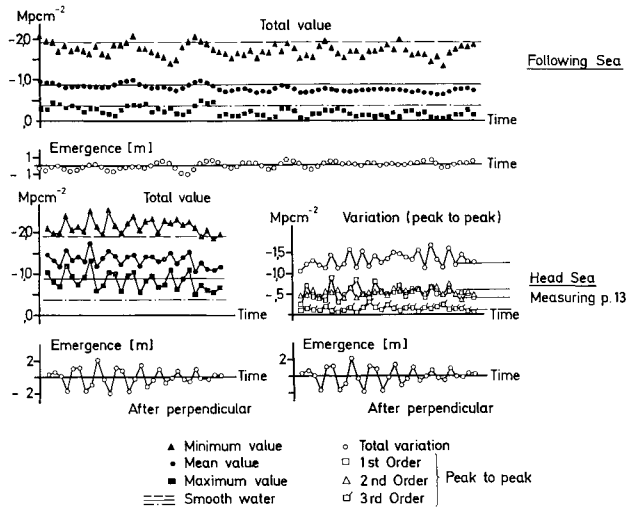

Fig. 9 Results of model tests in irregular seaway.

In this case the density and the torque coefficient K_Q were the same for both the model and the full-scale propeller. It was therefore possible to extrapolate the model stresses to the full scale merely by multiplying them by the model scale λ. Inevitably there will still remain some scale effect of the wake due to the differences in the relative boundary-layer thicknesses of the model and the full-scale ship.

3. Results

References will be made to only a few of the results obtained from the model tests. Figure 8 shows the results of the measurements obtained at the design draught compared with those obtained at the trials draught. The clusters of points at a speed corresponding to about $n = 135$ rpm are results that were obtained during tests performed to determine the reproducibility of the model tests. To some extent these indicate the scatter of the measurements made during the model tests.

In order to complete the picture of the stresses that might be set up in the propeller blades, additional stress measurements were made in a seaway. The results obtained at Point 13 during the course of tests in irregular waves are shown plotted against time in Fig. 9. Looking at the total values obtained in head seas it is apparent that the mean values of the stresses are some 40–50% higher than the corresponding smooth-water results, although the total variation is about the same. The modulation of the average value depends on the movements of the ship as indicated by the motions of the after perpendicular that are plotted as the bottom trace. The diagram showing the variations again clearly emphasizes the similarities of the values of the double ampli-

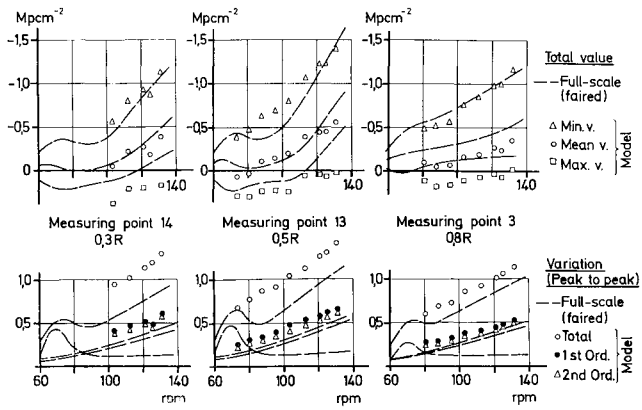

Fig. 10 Comparisons of model-test and full-scale results at $x = 0.3$, $x = 0.5$, and $x = 0.8$.

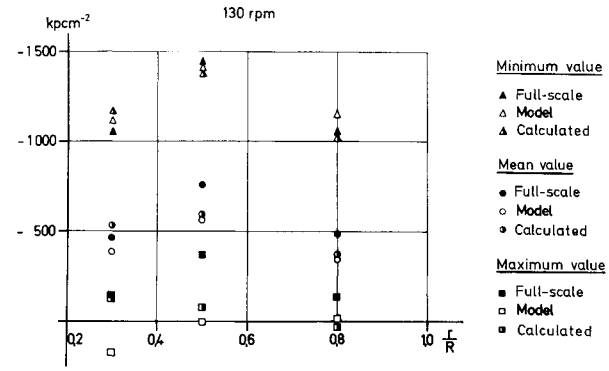

Fig. 11 Radial distribution of stresses at 130 rpm from calculation, model test, and full-scale test.

tudes (peak to peak) obtained in a seaway and in the smooth-water tests. The amplitudes of the individual harmonics of the stresses, of which only the first three are plotted to avoid confusing the records, vary considerably with time. This probably accounts for the rise and fall in the vibrations excited by the propeller that is known to occur in a seaway. It should be noted, incidentally, that these results are by no means merely of hypothetical nature, since the model seaway employed corresponded to a wind force of about $7\frac{1}{2}$ Beaufort, at which it is the practice for the ships to be driven at the full power of the machinery; this is the basis for the model tests which were carried out at a propeller speed corresponding to $n = 128$ rpm. The stresses in the propeller blades that were measured with the model running in a stern sea varied very little from the smooth-water results for the model seaway investigated.

Comparison of the Results of the Full-Scale Tests, Calculations, and Model Tests

In Fig. 10 the stresses obtained in the model tests are compared with the results of the trial trip of the full-scale ship. In this figure the separate points represent the model test results, and the interrupted lines are the fair lines through the full-scale results. A study of both the diagram giving the total values and the diagram showing the variations will prove that the converted values of the double amplitudes of the model are about 25–40% higher than the values obtained during the full-scale tests. This underlines the drawback of any model testing, namely the scale effect.

In Fig. 11 the radial stresses obtained from the full-scale trials, the model tests, and by calculation are shown plotted against the dimensionless propeller radius for the speed $n = 130$ rpm. Even though the scale effect is again clearly present, it is nevertheless clear that for certain purposes, such as the investigations in a seaway referred to above, stress measurements on the model can prove very useful. According to this diagram acceptable results can also be obtained from

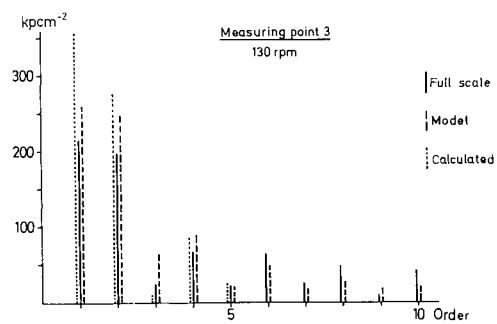

Fig. 12 Comparison of spectra.

calculations of the blade stresses based on forced vibrations with corrected loadings obtained from the two-dimensional aerofoil theory. As regards Fig. 12, which shows the spectrum of the harmonic orders for one speed and one measuring point, it may be remarked that the calculated values are closer to the model results than to the full-scale results.

The full-scale measurements have led to the conclusion that the propeller-blade fractures that have occurred were not caused by resonance effects. In fact the propeller blades were subjected to forced vibrations. With the exception of the speed range around 70 rpm the excitation is produced by the hull wake, the double amplitudes (peak to peak) of the stresses in this particular case amounting to about 150 percent of the average value. The fatigue limit of the material is then reached at a radius of $x = 0.5$. It is therefore necessary to make use of a fatigue diagram to assess the service strength of a marine propeller. In Fig. 13, which is a Haigh fatigue diagram, the value of $\sigma_w = 13.5$ kp/mm^2 plotted on the ordinate is the fatigue limit for 20×10^6 load cycles in a sea-water spray, and the value of $\sigma_F = 24.7$ kp/mm^2 plotted on the abcissa is the yield point in air. These values were determined by the propeller manufacturer from specimens taken from the material of the broken spare propeller.[2] Also plotted on the Haigh diagram is the maximum stress measured at radius $x = 0.5$ during the full-scale tests, less the average stress, plotted against this average stress. Since it was found in Fig. 10, which compared the full-scale and the model test results, that there was a sufficient agreement between these two values, it seems reasonable to include the model test results in a discussion of the propeller loading. Also plotted on Fig. 13 is therefore the arithmetic mean of five maximum values for the speed $n = 135$ rpm measured with the model run at the design draught. These five stress values, which have been previously shown on Fig. 8, produce a result which is definitely in excess of the fatigue limit. A consideration of the maximum stress values in a seaway would provide a complete explanation for the rapid failure of the propeller blades after only 4×10^6 or 8×10^6 load cycles. Frequency estimates for the various sea states have not yet been carried out for the routes on which the "Lichtenfels"-class ships are engaged. Therefore, these values have not been included on the loading diagram.

Conclusions

From the results reported in this paper, and especially from their use in a fatigue diagram, it is apparent that propeller-blade fractures could well be avoided even using the information and methods available to the practical designer. The comparison with the full-scale results shows that model tests and calculations of the stresses in the propeller blades, based on the wake field measured on the model, would prove to be very useful. It must, however, be borne in mind that a true indication of the safety margin available in practice will be obtained only if one compares the actual stresses and their variations with the fatigue limit of the material. A comparison of the mean stresses with the ultimate strength of the material would be of no use. The knowledge of the fatigue limit and of the yield point of the material in seawater is essential.

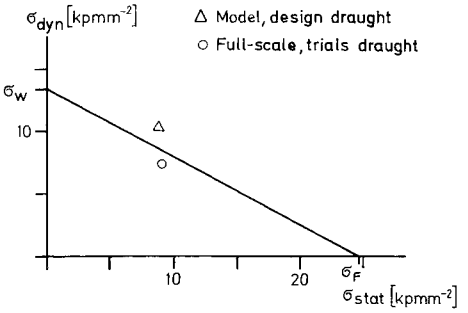

Fig. 13 Haigh diagram.

References

[1] Keil, H. G. and Weitendorf, E. A., "Fluegelschwingungsmessungen auf MS Neuenfels," *Schiff und Hafen*, Vol. 22, No. 4, April 1970, pp. 378–381.

[2] "Dehnungsmessungen an dem Propeller eines Einschrauben-Frachtschiffes mit 7200 PSe," Rept. 16/70, Nov. 1970, Forschungszentrum des Deutschen Schiffbaus, Hamburg, Germany (unpublished).

[3] Krohn, J., "Numerische und experimentelle Untersuchungen ueber die Abhaengigkeit der Schub- und Drehmomentenschwankungen vom Flaechenverhaeltnis bei vierfluegeligen Schiffspropellern," *Schiffstechnik*, Vol. 9, No. 48, Sept. 1962, pp. 181–188.

[4] Krohn, J., "Numerische und experimentelle Untersuchungen ueber die Abhaengigkeit der erregenden Querkraft und Biegemomentschwankungen vom Flaechenverhaeltnis bei fuenffluegeligen Schiffspropellern," *Schiffstechnik*, Vol. 10, No. 52, June 1963, pp. 83–92.

[5] Schwanecke, H., "Zur Frage der hydrodynamisch erregten Schwingungen von Schiffsantriebsanlagen," *Schiffstechnik*, Vol. 10, No. 54, Nov. 1963, pp. 155–169, also: Vol. 11, No. 55, Feb. 1964, pp. 10–26, and Vol. 11, No. 56, April 1964, pp. 39–60.

[6] Breslin, J. P., "Theoretical and Experimental Techniques for Practical Estimation of Propeller-Induced Vibratory Forces," *Symposium on Ship Vibration*, New York Metropolitan Sect. of Society of Naval Architects and Marine Engineers, Feb. 1970.

[7] Pfuetzner, H., "Theoretische Untersuchungen der Schwingungsbeanspruchung in Schiffspropellerfluegeln," *Schiff und Hafen*, Vol. 22, No. 3, March 1970, pp. 292–293.

[8] Boese, P., "Berechnungen der Biegeschwingungen des Propellerblattes unter Beruecksichtigung des Steigungsverlaufes ueber dem Radius," *Schiff und Hafen*, Vol. 22, No. 3, March 1970, pp. 294–296.

[9] Blume, P., "Berechnung der gekoppelten Biege- und Torsionsschwingungen des Propellerblattes unter Beruecksichtigung des Steigungsverlaufes ueber dem Radius," Rept. 266, Feb. 1971, Institut fuer Schiffbau of Hamburg University, Hamburg, Germany.

[10] Conolly, H. E., "Strength of Propellers," *Transactions of Royal Institution of Naval Architects*, Vol. 103, 1961, pp. 139–160.